

Predicted Effect Of Flowrate And Cooling Temperature On Horizontal Round Tube Absorber Of A Pair Working Fluid NH₃-H₂O

Nghia-Hieu NGUYEN¹⁾, Hiep-Chi LE²⁾, Quoc-An HOANG³⁾

^{1), 2)} Department of Heat & Refrigeration, Ho Chi Minh City University of Technology
Address: 268 Ly Thuong Kiet street, district 10, Ho Chi Minh, Vietnam.

³⁾ Research and International Relations Office, Ho Chi Minh City University of Technology and Education
Address: 1 Vo Van Ngan street, district Thu Duc, Ho Chi Minh, Vietnam.

Abstract: The performance of the absorption refrigeration system depends much on the absorber. The falling film absorption and bubble absorption studies performed experimentally and numerically for completed absorbers. This paper focuses on evaluating the parameters affecting the coupled heat-mass transfer as NH₃-H₂O diluted solution flowing on horizontal round tubes absorbs NH₃ vapor to become the stronger concentrated solution. The fields of velocity, temperature, concentration and thickness of the falling film solution varied by the input conditions of diluted solution and cooling water temperature flowing in the tube represented by a test volume element of the tube. The two-dimensional numerical simulation is written by the Matlab programming language to solve partial differential equations predicting absorption efficiency while changing the parameters affecting the absorption process.

Keywords: Absorption process, NH₃-H₂O solution, falling film on round tube

Nomenclature

x- Tangential coordinate along solution flow direction (m)
y- Local radial coordinate normal to solution flow direction (m)
ε- Non-dimensional tube half-circumference
η- Non-dimensional film thickness
u- Circumferential velocity (m/s)
v- Normal velocity (m/s)
δ- Film thickness (m)
ω- Solution concentration
T- Temperature (K)
α_{ib}- Convective heat transfer coefficient from interface to bulk (W/m² K)
α_{bw}- Convective heat transfer coefficient from bulk to wall (W/m² K)
α_{iw}- Heat transfer coefficient from interface to wall (W/m² K)
α_w- Convective heat transfer coefficient of cooling water (W/m² K)
U- Total heat transfer coefficient from film to water (W/m² K)
h_m- Mass transfer coefficient from interface to bulk (m/s)
h_{ab}- The heat of absorption (J/kg)
ν- Kinetic viscosity (m²/s)
WR- wetted ratio (%)
θ- Angle (radian)

I. Introduction

The performance of the absorption refrigeration system depends on the absorber. Heat and mass transfer processes occurring between liquid and vapor phases are key points in sizing and designing the absorber [1], [2]. This research focuses on the properties of motion, the coupled heat and mass transfer of falling film absorption on the horizontal tubes of the cooling tube bundle. Heat transfer coefficient, mass transfer coefficient, the distribution of solution concentration profile and temperature profile of the film leaving out the cooling tube bottom having decisive role in appropriate choice between adequate size of absorbers design and system operation base on the influence of fluid flow, coolant temperature, solution concentration inlet, and tube diameter... Falling film absorber is the most popular due to many advantages of heat transfer efficiency, easy to assemble, easy to manufacture, especially well-suited to Vietnam conditions. Therefore, the study of absorption

properties of the falling film and parameters influencing on cooling performance are urgently needed for accurate thermal calculations and applications for the design, manufacture, optimized operation.

Two common pairs of working fluid (refrigerant-absorbent) of refrigeration absorption systems are H₂O-LiBr and NH₃-H₂O. Testing absorber is using dilute NH₃-H₂O solution concentration distributed evenly from top to form the falling film around the tubes of parallel tube layers, NH₃ vapor go pass through the tube layers from the absorber bottom [4]-[9]. Dilute solution absorb NH₃ vapor to become stronger solution generating the absorbing heat flow. This heat flow go through the tube wall to the cooling water flowing in tubes and carrying it away. The falling film covers only one part of the tube depends on the fluid distribution along the tube length and surface tension of the solution, as well as surface roughness of tube.

II. Mathematical Model For A Test Volume

2.1. Model description

A test volume element has 100% wetted ratio. 3D physical models become 2D physical model has dilute solution flow direction along the tube circumference by coordinate x. Film thickness direction is from the tube center by coordinate y. Any points on the film are determined by coordinate θ , y respectively.

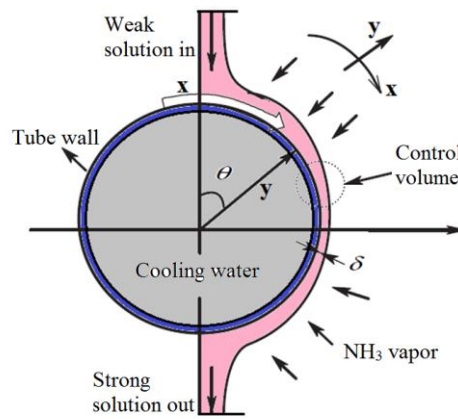


Fig.1. 2D physical model

Assumptions of 2D physical model

1. The flow is laminar and there are no interfacial waves;
2. Wettability of the solution on the tube surface is 100%;
3. Thermodynamic equilibrium exists at the interface between of solution film and vapor;
4. Heat transfer from interface to vapor phase is negligible;
5. The variation of film thickness due to absorption of NH₃ vapor is negligible;
6. Outside tube surface temperature equals the coolant temperature.

2.2. Mathematical description

The continuity, momentum, energy, transport equations of the solution falling film on the tube bundle are described 2D [1]-[13].

For a given solution mass flow rate per unit tube length $\Gamma = \frac{\dot{m}}{2 \cdot L_{tube} \cdot N_{tube}}$. Film thickness is expressed as equation (1).

$$\delta = \left[1 \frac{3v\Gamma}{(WR)\rho g \sin\theta} \right]^{1/3} \quad (1)$$

The velocity component u along x direction is belong to flow direction as equation (2).

$$u = \frac{g \sin\theta}{2\nu} (2\delta y - y^2) \quad (2)$$

The velocity component v along y direction is normal to flow direction as equation (3).

$$v = -\frac{g}{2\nu} y^2 \left[\frac{d\delta}{dx} \sin\theta + \frac{1}{R_o} \left(\delta - \frac{y}{3} \right) \cos\theta \right] \quad (3)$$

The phenomenon of coupled heat and mass transfer insteady state is discribed by the energy transport equation (4) and the species transport equation (5).

$$u \frac{\partial T}{\partial x} + v \frac{\partial T}{\partial y} = \alpha \frac{\partial^2 T}{\partial y^2} \quad (4)$$

$$u \frac{\partial \omega}{\partial x} + v \frac{\partial \omega}{\partial y} = D \frac{\partial^2 \omega}{\partial y^2} \quad (5)$$

Concentration and temperature boundary conditions at the inlet (6).

$$\begin{cases} x = x_{in} \\ 0 \leq y \leq \delta \end{cases} \rightarrow \begin{cases} T = T_{in} \\ \omega = \omega_{in} \end{cases} \quad (6)$$

Concentration and temperature boundary conditions on the tube wall surface (7).

$$\begin{cases} x_{in} \leq x \leq x_{out} \\ y = 0 \end{cases} \rightarrow \begin{cases} T = T_{wall} \\ \frac{\partial \omega}{\partial y} = 0 \end{cases} \quad (7)$$

Concentration and temperature boundary conditions at the liquid-vapor interface (8, 9, 10).

$$\begin{cases} x_{in} \leq x \leq x_{out} \\ y = \delta \end{cases} \rightarrow \begin{cases} \dot{m} = \frac{\rho D}{(1 - \omega_{int})} \frac{d\omega}{dy} aty = \delta (concentration)(8) \\ q = m' h_{ab} = k_f \frac{dT}{dy} aty = \delta (heatflow)(9) \\ T_{int} = f(p, \omega_{int}) aty = \delta (equivalent)(10) \end{cases}$$

The local heat transfer coefficients from the interface to bulk solution along the film flow (11) and from the bulk solution to tube wall surface along the film flow (12) in terms of Nusselt number.

$$Nu_{ib} = \frac{\alpha_{ib} \delta}{k_f} = \frac{\delta}{(T_{int} - T_{sb})} \frac{dT}{dy} aty = \delta \quad (11)$$

$$Nu_{bw} = \frac{\alpha_{bw} \delta}{k_f} = \frac{\delta}{(T_{sb} - T_w)} \frac{dT}{dy} aty = 0 \quad (12)$$

The mass transfer coefficient from the interface to bulk solution along the film flow (13) in terms of Sherwood number.

$$Sh = \frac{h_m \delta}{D_{ab}} = \frac{m' \delta}{D_{ab} \rho (\omega_{int} - \omega_{sb})} \quad (13)$$

The total heat transfer coefficient from the interface to cooling water flow can be expressed as (14) [2], [3].

$$\frac{1}{U} = \frac{1}{\alpha_{iw}} + \frac{1}{\alpha_w} + \frac{\delta_{wall}}{\lambda_{wall}} \quad (14)$$

The physical domain has a complex geometry. Moreover, the film thickness is in micro-size vs the half circumference length 0.0157m. This ratio make the domain can not be meshed directly which must be transformed from sliding coordinate xy to non-dimensional coordinate $\eta\zeta$ making the computational domain rectangular.

III. Result And Discussion

The parameters used in this study are presented in Table 1 [10]. Figures 2 to 8 show the dynamic characteristics of falling film and the coupled heat and mass transfer phenomenon as NH_3 vapor is absorbed in order to become a stronger concentrated solution.

Table 1. Input parameters

Parameters	Values
Inlet solution temperature T_{in}	316.15K
Inlet solution concentration ω_{in}	0.295
Absorber pressure p	2.88bar
Solution density	880kg/m ³
Dynamic viscosity μ	3.958*10 ⁻⁴ N.s/m ²
Solution flow rate Γ	0.005kg/(m.s)
Out tube radius R_o	0.005m
Thermal diffusivity α	6.7*10 ⁻⁸ m ² /s
Mass diffusivity D	4.4*10 ⁻⁹ m ² /s
Wall tube temperature T_{wall}	303.15K
Thermal conductivity of solution k_f	0.384W/(m.K)

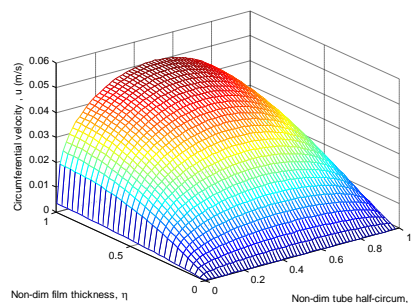


Fig. 2. Velocity u (m/s)

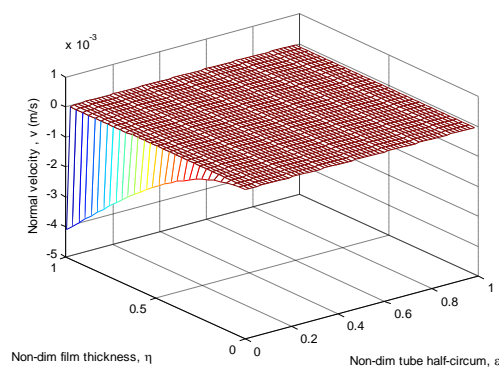


Fig. 3. Velocity v (m/s)

Figure 2 & 3 are the three-dimensional distribution of circumferential velocity component u and normal component v . According to dimensionless coordinate ϵ , in the first step, the liquid film falls into the tube so the velocity $u=0$; but velocity v very large and negative because it opposes the y -axis direction. When the film is formed on the tube, component u appears and grows. At $\epsilon=1/4$ tube u is maximum ($u_{\max}=0.0504\text{ m/s}$), then decreases and $u=0$ when flowing out of the tube. Y -axis, the velocity distribution of the component $u=0$ at the tube wall, increases gradually, and gets local maximum at the liquid-vapor interface. In contrast to u , component v after getting in the tube wall will decrease sharply, then increase sharply when going out of the tube.

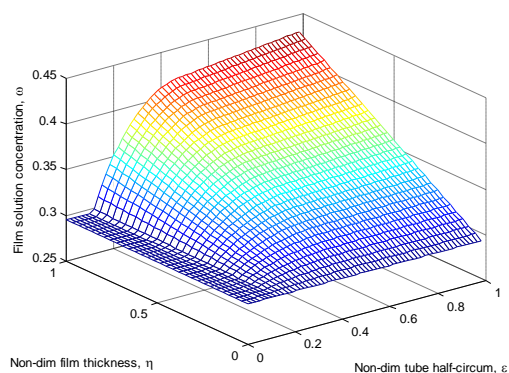


Fig. 4. Film solution concentration, ω

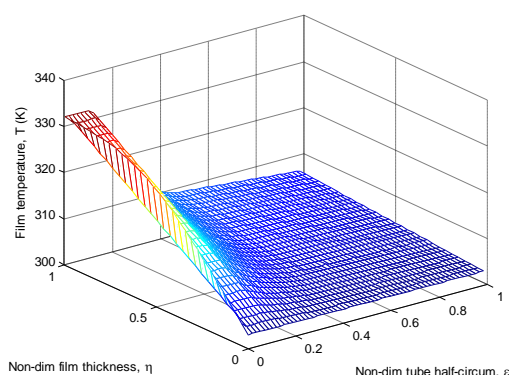


Fig. 5. Film temperature profile, T (K)

Figure 4 & 5 is the three-dimensional distribution of the concentration (ω), and temperature (T) in the solution film domain. The concentration of dilute solution when the solution has not contacted the tube assuming without absorption phenomenon so the concentration equals the inlet concentration. The interface temperature is saturated to solution concentration. At tube wall, solution temperature equals wall temperature. When absorption phenomenon occurs, the concentration of the liquid-vapor interface increases along ϵ -axis (x), then diffuses into the tube wall along η -axis (y). This absorption generates heat making liquid-vapor interface

temperature increases along ε -axis (x). Due to temperature difference between the interface and tube wall, the heat transfer to the wall along axis η (y).

The average concentration of the film leaves the wall $\omega = 0.3637$; increased 0.0687. The average temperature of the film come in the tube is 317.6K (44.5°C), the average temperature of the filmleave tube $T = 304.843K$ (31.7°C), decreased 12.8°C. The temperature of the liquid-vapor interfacecome in the tube is 332K (58°C), the temperature of the liquid-vapor interface leaves the tube is $T = 306.5K$ (33.4°C), decreased 24.7°C. Difference temperature between liquid-vapor interfaceleaving the tubeand the tube wall is 3.4°C.

Input data is in Table 1, the tube wall temperature is 303.15K, average local temperature at the inlet of falling film on tube is 332.1 K; changesolution flow rate (Γ): 0.001; 0.005; 0.008; 0.0113; 0.0146; 0.03kg/(m.s). Figures 6, 7, 8, 9, 10, 11, 12 and Table 2 show the thickness variation, the average local velocities, the average local concentrations, the average local temperatures, the heat transfer coefficient of the film, the total heat transfer coefficient, the mass transfer coefficient of the film.

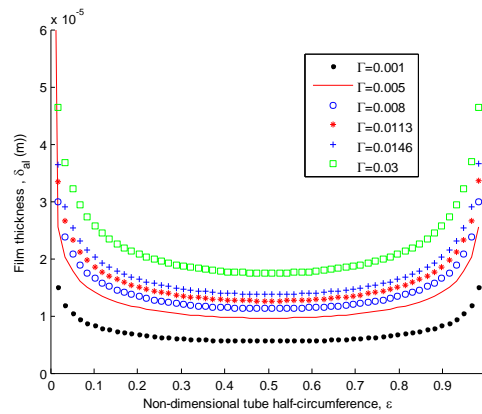


Fig. 6. Film thicness, δ (m)

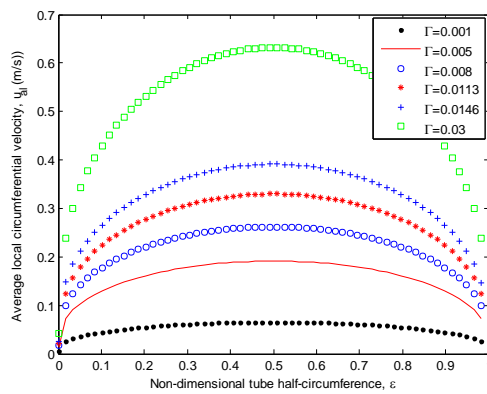


Fig. 7. Average local velocities, u_{al} (m/s)

When the solution flow rate decrease, the film thickness decrease (Figure 6), the circumferential velocity u decreases (Figure 7). At a quarter of the tube along flow direction, the film thickness is minimum, the film velocity is maximum.

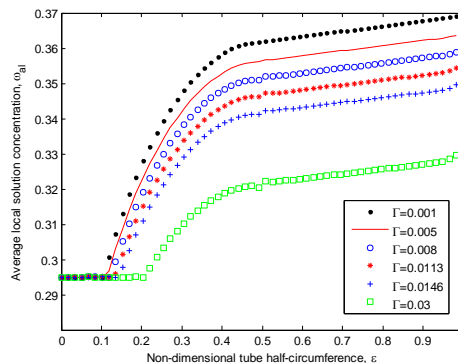


Fig. 8. Average local concentrations, ω_{al}

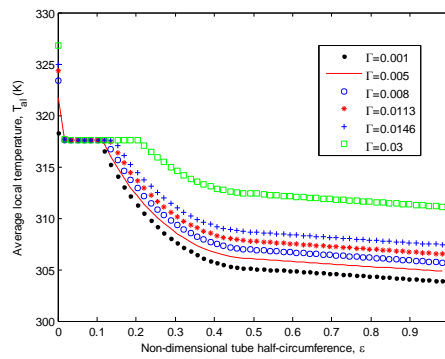


Fig. 9. Average local temperatures, T_{al} (K)

When the solution flow rate increases, the average local concentrations decreases (Figure 8), the average local temperature increases (Figure 9).

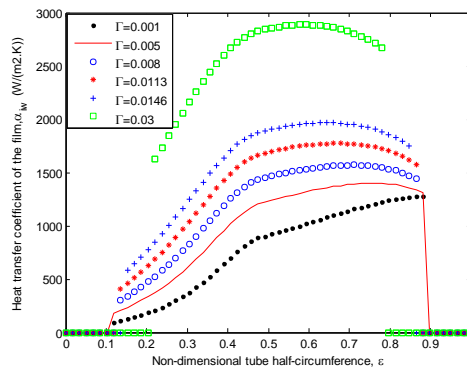


Fig. 10. Heat transfer coefficient of the film, α_{iw} ($W/m^2 K$)

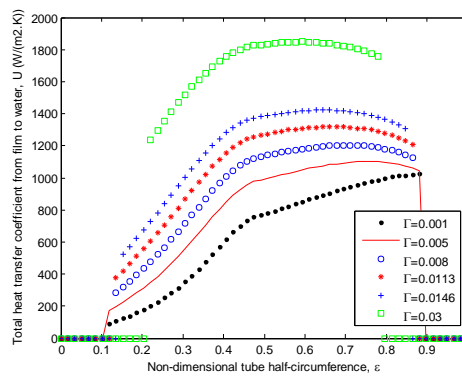


Fig. 11. Total heat transfer coefficient, U ($W/m^2 K$)

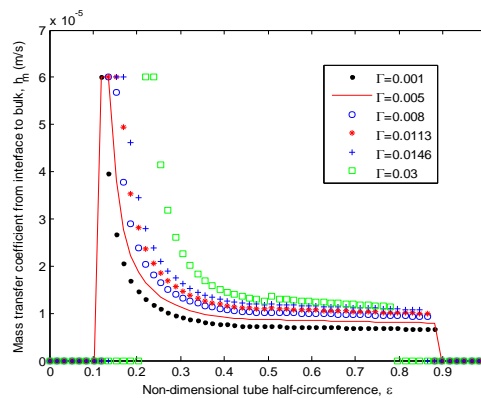


Fig. 12. Mass transfer coefficient of the film, h_m (m/s)

Figure 10 shows the change of the convective heat transfer coefficient of the film. Figure 11 shows the total heat transfer coefficient between the liquid-vapor interface and cooling water flowing in the tube U along ε -axis (x). These coefficients increase in the first quarter of the tube and decrease in the second quarter of tube shows absorption rate decreases as the heat transfer coefficient decreases. Solution flow rate increases, heat transfer coefficient increased strongly.

Figure 12 shows the change of the mass transfer coefficient along ε -axis (x). The mass transfer coefficient increase rapidly to the location where the dilute solution has just contact the tube wall; then decreased rapidly and fairly flat before leaving the tube wall. When the solution flow rate increases, the mass transfer coefficient increase, when increasing of flow rate is sizable $\Gamma = 0.0146\text{kg}/(\text{ms})$ or more, the mass transfer increase very small.

Table 2. Effecting of solution flow rate to heat and mass transfer process

$\Gamma/\text{kg}/(\text{ms})$	$\Gamma_{\text{ai}}(\text{out})$	$T_{\text{ai}}\text{K}(\text{out})$	$h_{\text{iw}} \cdot 10^3 \text{W}/(\text{m}^2\text{K})$	$U \cdot 10^3 \text{W}/(\text{m}^2\text{K})$	$h_{\text{m}} \cdot 10^{-4} \text{m}/\text{s}$
0.001	0.3690	303.9	0.7826	0.6578	0.1060
0.005	0.3636	304.8	1.0093	0.8221	0.1304
0.008	0.3589	305.7	1.2060	0.9567	0.1455
0.0113	0.3543	306.5	1.4010	1.0806	0.1600
0.0146	0.3495	307.4	1.6081	1.2068	0.1683
0.03	0.3297	311.1	2.5984	1.7169	0.1816

Input data is in Table 1, solution flow rate distribution $0.0146\text{kg}/(\text{ms})$, changes in tube wall temperature 311.15; 309.15; 307.15; 305.15; 303.15; 301.15K. Figures 13 and 14 represent average local concentrations, the average local temperatures. Table 3 shows the film thickness variation, the average local velocities, average local concentrations, the average local temperatures, film heat transfer coefficients, total heat transfer coefficients, mass transfer coefficients of the film.

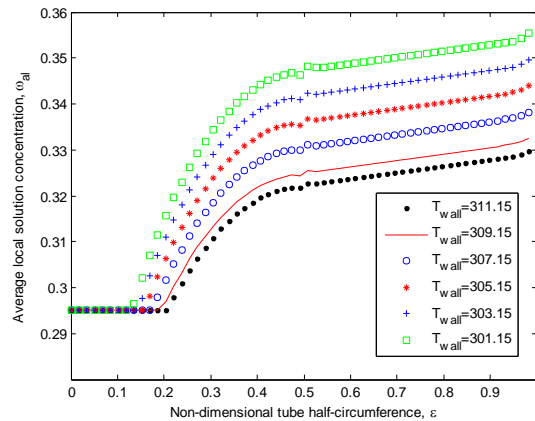


Fig. 13. Average local concentrations, ω

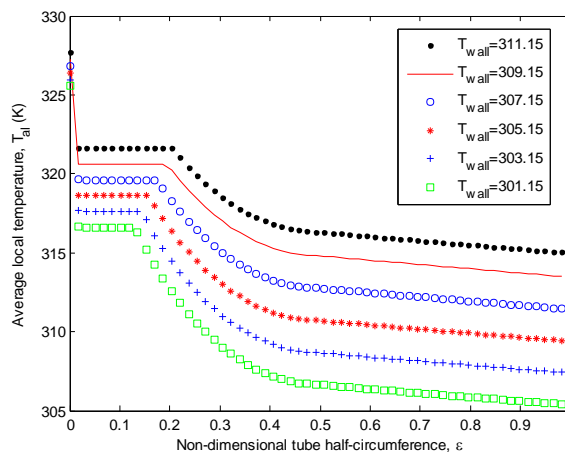


Fig. 14. Average local temperatures, T (K)

When the coolant temperature decreases, the average local concentration increases (Figure 13), the average local temperature decreases (Figure 14).

Table 3. Effecting of cooling water temperature to heat and mass transfer

T _{wat} (K)	ω _{ai} (out)	T _{ai} (K) (in/out)	h _{iw} .10 ³ W/(m ² K)	U.10 ³ W/(m ² K)	h _m .10 ⁻⁴ m/s
311.15	0.3298	321.6/315	1.4409	1.1165	0.1443
309.15	0.3325	320.6/313.5	1.4823	1.1407	0.1570
307.15	0.3382	319.6/311.5	1.5283	1.1657	0.1693
305.15	0.3440	318.6/309.4	1.5703	1.1878	0.1804
303.15	0.3497	317.6/307.4	1.6070	1.2062	0.1901
301.15	0.3554	316.6/305.4	1.6424	1.2233	0.1989

According to Table 3, the cooling water temperature decreases, the average concentration of the film leave the tube increases, the average film temperature leave the tube decreases. Cooling water temperature decreases, the heat transfer coefficient of the film and total heat transfer coefficient increase very little; mass transfer coefficient increases significantly.

IV. Conclusion

1. Solution flow rate distribution $\Gamma = 0.005 \text{ kg/(ms)}$. Velocity component u appear and grow, get maximum at $1/4$ tube ($u_{\text{max}} = 0.0504 \text{ m/s}$) while the velocity component v is smallest and film thickness is minimum $\delta_{\text{min}} = 0.0096 \cdot 10^{-3} \text{ m}$ along the flow. The average concentration of the film leaving the tube $\omega = 0.3637$; increased 0.0687 . The average temperature of the film leaving the tube $T = 304 \text{ K}$ (31°C), decreased 12.8°C . The liquid-gas interface temperature leaving the tube $T = 306.54 \text{ K}$ (33.4°C), decreased 25.6°C . The difference temperature of the liquid-vapor interface leaving the tube and the tube wall temperature is 3.4°C . Heat transfer coefficient of the film $\alpha_{iw} = 744 \text{ W/(m}^2 \text{K)}$. The total heat transfer coefficient from liquid-vapor interface to the cooling water $U = 640 \text{ W/(m}^2 \text{K)}$. The average mass transfer coefficient $h_m = 1.4699 \cdot 10^{-5} \text{ m/s}$ along the x -axis.
2. Solution flow rate increases, the average local concentrations of the film decrease (Fig. 8), average local temperature increases (Fig. 9); heat transfer coefficient increase strongly, mass transfer coefficient increase. When increasing of flow rate is sizable $\Gamma = 0.0146 \text{ kg/(ms)}$ or more, the mass transfer increase very small, according to table 2.
3. Cooling water temperature decreases, the average concentrations of the film leave the tube increases, the average temperatures leave the tube decrease. Cooling water temperature decreases, the heat transfer coefficients of the film and overall heat transfer coefficients increase very small; mass transfer coefficients increase significantly according to table 3.

References

- [1]. Nomura, T., N. Nishimura, S. Wei and S. Yamaguchi. Heat and Mass Transfer Mechanism in the Absorber of H₂O/LiBr Conventional Absorption Refrigerator: Experimental Examination by Visualized Model, International Absorption Heat Pump Conference, AES–vol. 31, pp.203–208. 1993.
- [2]. Islam, M.R., N.E. Wijesundera and J.C. Ho. Simplified models for coupled heat and mass transfer in falling-film absorbers, Int. J. of Heat and Mass Transfer., vol. 47(2), pp. 395–406. 2004
- [3]. Oosthuizen, Patric H. and David Naylor. Edwards, Convective Heat Transfer Analysis, pp. 5756–577, McGraw-Hill International Editions, 1999.
- [4]. Islam, M.R., N.E. Wijesundera and J.C. Ho. Simplified models for coupled heat and mass transfer in falling-film absorbers, Int. J. of Heat and Mass Transfer, vol. 47(2), pp. 395–406, 2004.
- [5]. Hu, X. and A.M. Jacobi. Departure-site spacing for liquid droplets and jets falling between horizontal circular tubes, Experimental Thermal and Fluid Science, Vol. 16, p. 322–331, 1998.
- [6]. Killion, J.D. and S. Garimella. Gravity-driven Flow of Liquid Films and Droplets in Horizontal Tube Banks, International Journal of Refrigeration, vol. 26, p. 516–526, 2003.
- [7]. Frances, V.M.S. and J.M.P. Ojer. Validation of a Model for the Absorption Process of H₂O (vap.) By a LiBr(aq.) in a Horizontal Tube Bundle, Using Multi-factorial Analysis, International Journal of Heat and Mass Transfer, vol.46(17), pp.3299–3312. 2003.
- [8]. Islam, M.R., N.E. Wijesundera and J.C. Ho. Evaluation of Heat and Mass Transfer Coefficients for Falling-Films on Tubular Absorbers, Int. J. Refrigeration, vol. 26, p. 197–204, 2003.
- [9]. Jesse D. Killion, SrinivasGarimella. Pendant droplet motion for absorption on horizontal tube banks. International Journal of Heat and Mass Transfer 47 p. 4403–4414, 2004.
- [10]. Conlisk AT, Mao J, “Nonisothermal absorption on a horizontal cylindrical tube-1. The film flow”, Chemical engineering science, 51, p. 1275–1285, 1996.
- [11]. Md. Raisul Islam, “Absorption process of a falling film on a tubular absorber: An experimental and numerical study”, Applied Thermal Engineering 28, p. 1386–1394, 2008.
- [12]. V.D. Papaefthimiou, I.P. Koronaki, D.C. Karampinos, E.D. Rogdakis, “A novel approach for modelling LiBr- H₂O falling film absorption on cooled horizontal bundle of tubes”, Int. J. of refrigeration 35, p. 1115–1122, 2012.
- [13]. L. Harikrishnan, Shaligram Tiwari*, M.P. Maiya, “Numerical study of heat and mass transfer characteristics on a falling film horizontal tubular absorber for R-134a-DMAC”, International Journal of Thermal Sciences 50, p. 149–159, 2011.